Synergistic Flame-Retardant Effect of DOPO-Based Derivative and Modified Sepiolite on Flame Retardancy, Thermal Decomposition and Mechanical Properties of PEO/PBAT Blends

Weijiang Huang *, Chunyun Tu, Qin Tian, Kui Wang, Chunlin Yang, Chao Ma, Xiaolu Xu, Wei Yan *

Posted Date: 9 November 2023

doi: 10.20944/preprints202311.0666.v1

Keywords: poly (ethylene oxide); poly (butylene adipate-co-terephthalate); DOPO-based flame retardant; sepiolite; synergistic effect

Article

Synergistic Flame-Retardant Effect of DOPO-Based Derivative and Modified Sepiolite on Flame Retardancy, Thermal Decomposition and Mechanical Properties of PEO/PBAT Blends

Weijiang Huang [1, 2, *], Chunyun Tu [1], Qin Tian [1, 2], Kui Wang [1], Chunlin Yang [1], Chao Ma [1], Xiaolu Xu [1], Wei Yan [1, 2,*]

[1] School of Materials Science and Engineering, Guiyang University, Guiyang 550005, China; yidapa@sina.cn (C. T.); mabtianqin@126.com (Q. T.); gyxywkui@163.com (K. W.); ycl770309@163.com (C. Y.); chaomagyu@126.com (C. M.); gyxyxxl@126.com (X. X.)

[2] National Engineering Research Center for Compounding and Modification of Polymer Materials, Guiyang 550014, China

* Correspondence: huangweijiang_2007@126.com (W. H.); lrasyw@163.com (W. Y.)

Abstract: A bridged 9,10-dihydro-9-oxa-10-phosphaphenanthrene-10-oxide (DOPO) derivative (PN-DOPO) in combination with aluminum phosphates coated sepiolite (Sep@$AlPO_4$) was used to improve the flame retardancy, thermal stability and mechanical properties of poly (ethylene oxide) (PEO)/poly (butylene adipate-co-terephthalate) (PBAT) blends. The synergistic effects of PN-DOPO and Sep@$AlPO_4$ on the fire resistance, thermal decomposition behavior and mechanical properties of PEO/PBAT composites were investigated systematically. The results indicated that 5 wt % Sep@$AlPO_4$ combined with 10 wt% PN-DOPO into PEO/PBAT achieved a V-1 rating in UL-94 test and the LOI value increased to 23.7%, meanwhile, the peak-heat release rate (p-HRR), av-HRR and total heat release (THR) values of PEO/PBAT/PN10%/Sep5% composites decreased by 35.6%, 11.0% and 23.0% compared with those of PEO/PBAT, respectively. The thermogravimetric analysis (TGA) results confirmed that PN-DOPO/Sep@$AlPO_4$ could enhance the initial thermal stability and char yield of PEO/PBAT matrix, and TGA/Fourier transform infrared spectrometry (TGA-FTIR) results revealed that the composites exhibited the absorption peaks of phosphorous-containing groups and an increase in gas-phase volatiles during the thermal decomposition process. The digital photographs and morphological structures of char residues demonstrated that PN-DOPO and Sep@$AlPO_4$ mixtures benefited to the formation of a more continuous and dense carbon layer on the composites surface during combustion. Rheological behavior revealed that a higher storage modulus, loss modulus and complex viscosity of PEO/PBAT/PN-DOPO/Sep@$AlPO_4$ composites could also promote the cross-linking structure during burning. Furthermore, the PEO/PBAT/PN-DOPO/Sep@$AlPO_4$ composites exhibited excellent mechanical properties in terms of elongation at break and flexural performance than the PEO/PBAT system. All the results demonstrated that PEO/PBAT system modified by the combination of PN-DOPO and Sep@$AlPO_4$ not only exhibited excellent synergistic effect on the flame retardance, but also had good improvement on thermal stability and mechanical properties, indicating the potential application in areas requiring fire safety.

Keywords: poly (ethylene oxide); poly (butylene adipate-co-terephthalate); DOPO-based flame retardant; sepiolite; synergistic effect

1. Introduction

Poly (ethylene oxide) (PEO) is typically used as a matrix for solid polymer electrolyte (SPE), as lithium salts are well soluble in PEO, thereby promoting the generation of charge carriers for conductive ions [1,2]. In addition, PEO can be used for synthesizing of water-soluble film and molding due to its low toxicity, good biological adhesion, good water solubility, and easy processing. However, the neat PEO has low thermal stability, poor mechanical strength and rheological

 doi:10.20944/preprints202311.0666.v1

properties at room temperature [3–5]. Therefore, blending PEO with other polymers is one of the effective means- to improve the shortcomings of PEO-based matrix.

In recent years, due to the increasing requirements of sustainability, green renewable and biodegradable, PEO-biopolymer blends can be considered as one of the research directions to improve the performance of matrix [6]. Poly (butylene adipate-co-terephthalate) (PBAT), as a fully biodegradable aliphatic-aromatic polyester, has been frequently mixed with other polymers due to its excellent elongation at break, good processing properties and hydrophilicity [7,8]. Thus, PBAT can be considered as a promising and practical counterpart for blending with PEO. Ye et al. [6] prepared PBAT/Poly (lactic acid) (PLA) based nano-composites by melt-mixing PLA and PBAT with freeze-dried PEO/Graphene nanoplatelets (GNP) masterbatch. It was found that a small amount of PEO incorporation could enhance the dispersion of GNP in the dispersed PBAT phase, improve greatly the toughness and thermal stability of nanocomposites.

However, both PEO and PBAT still encounter some safety hazards in terms of catching fire. On the one hand, although PEO and PBAT are widely used, the polymers themselves are easy to burn [9–12]. They have low limiting oxygen index (LOI, all less than 21%) with serious melt dripping during combustion. On the other hand, PEO-based solid polymer electrolyte usually operated at higher temperatures, such as more than 60 °C or even higher, which puts forward higher requirements for the thermal stability and flame retardancy of the PEO-based blends [13–15]. Therefore, in order to enhance the safety of the matrix and reduce the fire risk under high temperature conditions, high-performance PEO-based composites with excellent flame retardancy are very desirable. In this respect, little efforts have been devoted in designing blends to improve the flame retardancy and rheological properties of PEO-based composites [16].

Among many flame retardant，9,10-dihydro-9-oxa-10-phosphaphenanthrene-10-oxide (DOPO) and its derivatives have attracted much attention due to the outstanding flame retardancy and low toxicity in various polymers such as polyesters, epoxies, polyamides and cellulose [17–20]. According to our previous reports, a bridged DOPO (PN-DOPO) flame retardant was prepared and verified to exhibit excellent flame retardancy for polyamide, epoxy resin, polylactic acid and polyolefins [21–24]. To further improve the flame retardancy of DOPO-based flame retardants, the introduction of synergistic agents is usually considered. The most commonly used synergists mainly involve inorganic particles, such as graphite oxide, montmorillonite, sepiolite, halloysite and carbon nanotubes [25–27]. Among them, sepiolite as a natural silicate clay material with a unique nanofibrous structure, which makes it to be a potential flame retardant or reinforcing agent. However, when sepiolite is used as flame retardant alone, the flame-retardant performance is not prominent [28,29]. For these reasons, the organic-inorganic hybrid flame retardant was prepared by coating the sepiolite surface with aluminum phosphate (Sep@$AlPO_4$) via a simple precipitation strategy based on our previous reports [30]. The hybrid nanocomposite could enhance the flame retardancy of epoxy resin by forming thermally stable carbonaceous char and improve the mechanical performance and thermal stability of the matrix. These previous works made believed that the modified sepiolite could further enhance the flame-retardant efficiency and improve the its compatibility with the matrix.

In this work, PEO/PBAT/PN-DOPO/Sep@$AlPO_4$ composites were prepared by melt blending with PEO/PBAT as the matrix, self-made PN-DOPO as flame retardant and aluminum phosphate coated sepiolite as synergist. The synergistic flame-retardant effect, rheological behavior, thermal stability and mechanical performance of PN-DOPO combined with Sep@$AlPO_4$ on PEO/PBAT blend was systematically evaluated. The morphology and composition structure of char residues were characterized. Moreover, the possible synergistic effect of PN-DOPO and Sep@$AlPO_4$ on the flammability and rheological properties of flame-retarded PEO/PBAT blends were also discussed.

2. Materials and Methods

2.1. Materials

The PEO (M_w: 100,000) were supplied by Shanghai Macklin Biochemical Co., Ltd., Shanghai, China. The PBAT resin (M_n: 24,400 g/mol) was purchased from Shanxi Jinhui Zhaolong High-Tech

 doi:10.20944/preprints202311.0666.v1

Co., Ltd., Shanxi, China with a melt flow index of 5 g/10 min (180 °C, 2.16 kg) and density of 1.24 g/cm^3. The flame retardant (FR，PN-DOPO) and synergist (aluminum phosphates coated sepiolite, Sep@$AlPO_4$) were synthesized in the laboratory according to as per our previously reports [23,30,31].

2.2. Preparation of PEO/PBAT/PN-DOPO/Sep@$AlPO_4$ Composites

PEO, PBAT, PN-DOPO coupled with Sep@$AlPO_4$ were dried in a vacuum oven at 80 °C for 5 hours prior to compounding. PEO/PBAT/PN-DOPO/Sep@$AlPO_4$ composites were prepared by melt blending in a torque rheometer (Haake PolyLab OS, Thermo Fisher Scientific Co., Ltd., Karlsruhe, Germany) at 150 °C with a screw speed of 50 rpm for 6 min. Table 1 lists the composition and corresponding content of each sample. Then the mixtures were hot-pressed first at 150 °C for 10 min at 15 MPa. They were then cold-pressed at room temperature for 15 min with 15 MPa into sheets of suitable size and thickness using a plate vulcaniser (ZHY-W, Chengde Testing Machine Factory, Hebei, China) for flame retardancy and mechanical properties tests.

Table 1. Composition of the PEO/PBAT/PN-DOPO/Sep@$AlPO_4$ composites.

Samples	PEO (wt%)	PBAT (wt%)	PN-DOPO (wt%)	Sep@$AlPO_4$ (wt%)
PEO/PBAT	60	40	0	0
PEO/PBAT/PN15%	60	40	15	0
PEO/PBAT/PN14%/Sep1%	60	40	14	1
PEO/PBAT/PN12%/Sep3%	60	40	12	3
PEO/PBAT/PN10%/Sep5%	60	40	10	5
PEO/PBAT/PN8%/Sep7%	60	40	8	7
PEO/PBAT/Sep15%	60	40	0	15

2.3. Characterization

The UL-94 vertical combustion test was performed as per ASTM D3801 with the sample size of 130.0 mm × 13.0 mm × 3.2 mm. The LOI values were tested using LOI instrument according to ASTM D2863-06. The sample dimensions were 130.0 mm × 6.5 mm × 3.2 mm. The cone calorimeter tests were evaluated with an FTT cone calorimeter (Fire Testing Technology, East Grinstead, UK) exposing a radiant cone at a heat flux of 50 kW/m^2 according to ISO 5660-1 (the specimen size of 100.0 mm × 100.0 mm × 6.0 mm).

The thermal stability of samples was measured via thermogravimetric analysis (TGA) (TG 219 F3, Netzsch Instruments Co., Ltd., Selbu, Germany) in a nitrogen atmosphere at the flow rate of 60 mL/min. Each specimen (about 5-10 mg) was heated from 30 °C to 800 °C at a heating rateat of 10 °C/min.

The rheological properties of samples were obtained using a Rheometric Analyzer (HAAKE MARSII, Thermo Fisher Scientific Inc., Karlsruhe, Germany). The diameter of parallel plates was 35 mm. Dynamic frequency sweep tests were performed at 150 °C using 1% strain under an angular frequency range of 0.1–100 rad/s.

The morphology of the char residues after the cone calorimeter test was performed via SEM (Quanta FEG 250, FEI Instruments, USA) under an acceleration voltage of 20 kV. Energy dispersive spectrometry (EDS) (INCA-350, Oxford, UK) was analyzed by characterizing the chemical composition and morphology of the char residues after combustion. The EDS analyzes were recorded on a Quanta FEG 250 SEM equipped with an EDS accessory at the voltage of 30 kV.

The released gases after TGA at different temperatures were investigated by Fourier transform infrared (FTIR) spectra. The TGA-FTIR analysis was characterized using simultaneous thermogravimetry coupled with FTIR spectrometer (Nicolet iS50, Thermo Fisher Scientific Inc., Waltham, MA, USA). The evolved gases were transported to the FTIR spectrometer through a connecting line. The FTIR spectra were collected at a resolution of 4.0 cm^{-1} across a wave number range of 500-4000 cm^{-1}, and 16 scans were conducted for each sample.

 doi:10.20944/preprints202311.0666.v1

The mechanical properties of the composites were performed using CMT6104 universal testing machine (MTS Systems Co., Ltd., Shanghai, China). The tensile tests were measured as per ASTM D-638 using an extensometer at the crosshead of speed of 50.0 mm/min. The flexural tests were experimented as per ASTM D-790 at crosshead speed of 2.0 mm/min. For each sample, the reported results are the average of five specimens and the range of average deviations was within 5%.

3. Results and Discussion

3.1. Flame Retardancy of PEO/PBAT/PN-DOPO/Sep@AlPO₄ Composites

The LOI measurement and UL-94 test are widely used to evaluate the flame-retardant properties of polymers. Table 2 lists the corresponding experimental results. Due to the intrinsic dripping characteristics and the low LOI values of PLA and PBAT, the PEO/PBAT sample exhibited severe dripping during combustion, and the LOI value was merely about 20.2%. The recorded flame times were more than 30 s, and no rating was reached. When 15 wt% PN-DOPO was added to PEO/PBAT blend, the LOI value increased to 22.6% and a UL-94 V-2 rating was attained. For only 15 wt% Sep@AlPO₄ loading, the LOI value of PEO/PBAT/Sep15% was 21.8% and the composites also attained V-2 rating. The dripping phenomenon was still evident.

Table 2. The UL-94 vertical combustion and LOI tests of the PEO/PBAT/PN-DOPO/Sep@AlPO₄ composites.

Samples	UL-94 (3.2mm)				LOI (%)
	t_1 (s)	t_2 (s)	Dripping	Rating	
PEO/PBAT	> 30	> 30	Yes	No Rating	20.2
PEO/PBAT/PN15%	19.6	5.1	Yes	V-2	22.6
PEO/PBAT/PN14%/Sep1%	18.5	3.4	Yes	V-2	22.8
PEO/PBAT/PN12%/Sep3%	12.7	4.6	No	V-1	23.2
PEO/PBAT/PN10%/Sep5%	11.4	2.8	No	V-1	23.7
PEO/PBAT/PN8%/Sep7%	16.8	6.2	Yes	V-2	23.1
PEO/PBAT/Sep15%	20.1	5.5	Yes	V-2	21.8

Incorporating Sep@AlPO₄ into PEO/PBAT/PN-DOPO blends to further improve the flame-retardant efficiency. The loading of PN-DOPO/Sep@AlPO₄ compounds was maintained at 15 wt% in the PEO/PBAT samples. When 3 wt% and 5 wt% Sep@AlPO₄ replaced the same amount of PN-DOPO, respectively, the V-1 rating was reached and exhibited anti-dripping properties. Furthermore, the LOI value of PEO/PBAT/PN10%/Sep5% sample was increased to 23.7%. The flammability test results indicated that a synergistic flame-retardant effect occurred between PN-DOPO and modest addition of Sep@AlPO₄, and the combination could further improve the flame retardancy of PEO/PBAT blends.

3.2. Cone Calorimeter Tests

In order to further investigate the synergistic flame-retardant effect of PN-DOPO/ Sep@AlPO₄ compounds on PEO/PBAT system, the combustion behavior of PEO/PBAT/PN-DOPO/Sep@AlPO₄ composite was evaluated using a cone calorimeter test. The corresponding data are summarized in Table 3. The ignition time (TTI) is usually used to represent the duration before polymer combustion, and the higher TTI, it is more difficult to ignite under a luminous flame for polymer [32]. As shown in Table 3, the TTI of samples after incorporating PN-DOPO or PN-DOPO/Sep@AlPO₄ compounds obviously increased, compared with neat PEO/PBAT. Specifically, it was extended (about 17 seconds) when 10 wt% PN-DOPO and 5 wt% Sep@AlPO₄ were introduced into the PEO/PBAT system, and the composite had a TTI of 62 seconds. The increased in TTI suggested that the flame-retarded PEO/PBAT/PN-DOPO/Sep@AlPO₄ could delay the early stages of the composite decomposition process [33].

Figure 1 presents the heat release rate (HRR) and total heat release (THR) curves of flame-retarded PEO/PBAT composites. As showed in Figure 1, the PEO/PBAT burned violently after

Preprints (www.preprints.org) | NOT PEER-REVIEWED | Posted: 9 November 2023 doi:10.20944/preprints202311.0666.v1

ignition and reached a sharp p-HRR of 1021.4 kW/m². The p-HRR decreased to 815.7 kW/m² with the addition of 15 wt% PN-DOPO. When the amount of Sep@AlPO₄ was 15 wt%, the p-HRR reached 851.6 kW/m². After incorporation 10 wt% PN-DOPO and 5 wt% Sep@AlPO₄ into PEO/PBAT, the p-HRR reached only 657.8 kW/m² and decreased by 35.6%. The time to p-HRR (T_{PHRR}) was also significantly delayed to 385 seconds of PEO/PBAT/PN10%/Sep5% compared to that of 354 seconds of PEO/PBAT. The increased in T_{PHRR} indicated that the PEO/PBAT/PN-DOPO/Sep@AlPO₄ composites were more difficult to burn or delay thermal decomposition than neat PEO/PBAT [7,30]. As listed in Table 3, the THR and average heat release (av-HRR) of PEO/PBAT were 218.5 MJ/m² and 574.3 kW/m², respectively. With the addition of PN-DOPO, the THR and aV-HRR values were clearly decreased. When PN-DOPO is partially replaced by Sep@AlPO₄, the THR and av-HRR values of PEO/PBAT/PN10%/Sep5% decreased by 11.0% and 23.0% compared with those of PEO/PBAT, respectively.

Table 3. Results of cone calorimeter tests for PEO/PBAT/PN-DOPO/Sep@AlPO₄ composites.

Samples	TTI (s)	p-HRR (kW/m²)	av-HRR (kW/m²)	T_{PHRR} (s)	THR (MJ/m²)	TSR (m²/m²)	av-COY (kg/kg)
PEO/PBAT	55	1021.4	574.3	354	218.5	579.0	0.04
PEO/PBAT/PN15%	61	815.7	486.0	359	194.2	3044.3	0.22
PEO/PBAT/PN10%/Sep5%	62	657.8	442.3	385	194.5	2094.1	0.18
PEO/PBAT/Sep15%	59	851.6	501.7	373	204.0	483.9	0.05

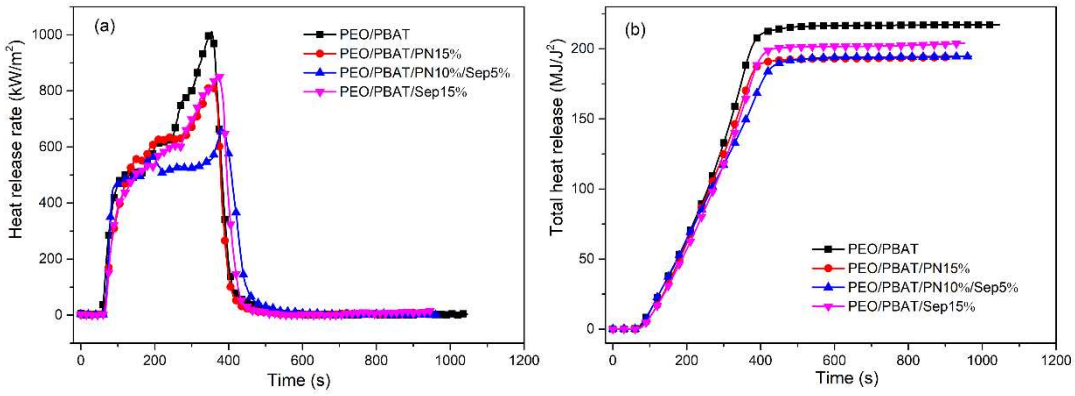

Figure 1. Heat release rate (a) and total heat release (b) curves of flame-retarded PEO/PBAT composites.

Smoke emission is another key parameter for evaluating the flame retardancy of polymers. The total smoke release (TSR) and carbon dioxide production curves are shown in Figure 2. As presented in Figure 2, the TSR value of PEO/PBAT was 579.0 m²/m². When 15 wt% PN-DOPO was added to PEO/PBAT, TSR value (3044 m²/m²) was apparently increased because of the more incomplete combustion [34]. After incorporation 10 wt% PN-DOPO and 5 wt% Sep@AlPO₄ into PEO/PBAT, the TSR was reduced to 2094 m²/m². The decrease in TSR might be attributed to the formation of more compact and thermally stable residues that serve as effective physical barriers [25]. It should be noted that the TSR values of PEO/PBAT/PN15% and PEO/PBAT/PN10%/Sep5% are significantly higher than that of PEO/PBAT or PEO/PBAT/Sep15%. Besides TSR values, PEO/PBAT/PN10%/Sep5% displayed the higher average COY value (0.18 kg/kg) and lower peak CO_2 production (0.36 g/s) than that of PEO/PBAT (0.04 kg/kg of COY and 0.62 g/s of CO_2 production), which might be due to incomplete combustion of flame-retarded composites with the addition of PN-DOPO and Sep@AlPO₄. The results of TSR, CO_2 production and av-COY also reveal that the incorporation of PN-DOPO/Sep@AlPO₄ into PEO/PBAT blends results in a notable gas-phase flame retardancy and synergistic smoke suppression effects [35].

Preprints (www.preprints.org) | NOT PEER-REVIEWED | Posted: 9 November 2023 doi:10.20944/preprints202311.0666.v1

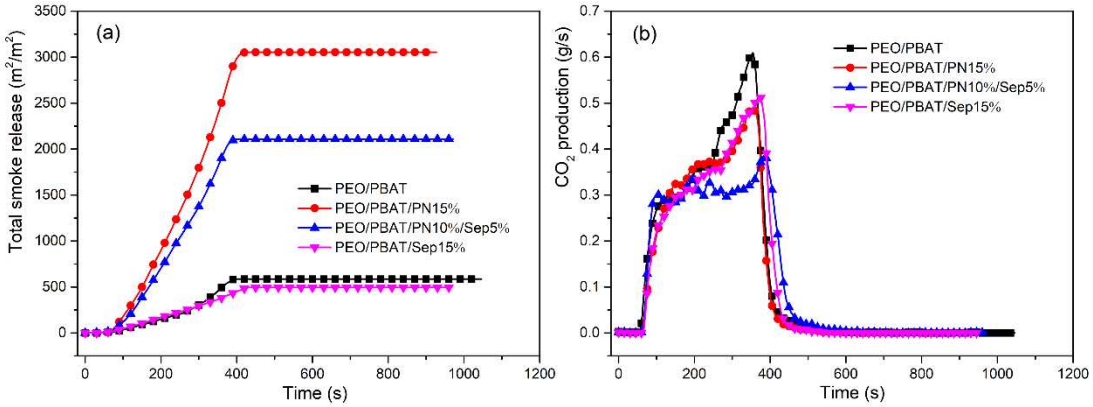

Figure 2. Total smoke release (a) and carbon dioxide production (b) curves of flame-retarded PEO/PBAT composites.

Based on the above analysis, the incorporation of PN-DOPO and Sep@$AlPO_4$ could further improve the flame retardancy of PEO/PBAT blends. In addition, it can be concluded that the combination of PN-DOPO and Sep@$AlPO_4$ exhibited remarkable synergistic flame-retardant and smoke suppression effects in flame-retarded PEO/PBAT composites.

3.3. Thermal Stability Analysis

The TGA and differential thermogravimetric analysis (DTG) curves of the samples in nitrogen atmosphere are presented in Figure 3, and the detailed parameters are listed in Table 4. The corresponding data included $T_{5\%}$, defined as the onset decomposition temperature at 5% mass loss, T_{max}, defined as the maximum decomposition temperature at the maximum mass loss rate, and the residue amount at 800 °C.

Table 4. TGA and DTG data of flame-retarded PEO/PBAT composites.

Samples	$T_{5\%}$ (°C)	T_{max} (°C)	The residues at 800 °C (wt%)
PEO/PBAT	344.9	409.5	0.06
PEO/PBAT/PN15%	357.5	409.7	1.86
PEO/PBAT/PN14%/Sep1%	347.7	407.2	0.62
PEO/PBAT/PN12%/Sep3%	363.4	410.7	3.54
PEO/PBAT/PN10%/Sep5%	361.8	408.1	4.76
PEO/PBAT/PN8%/Sep7%	357.0	406.4	9.18
PEO/PBAT/Sep15%	356.8	407.6	10.27

The thermal decomposition of PEO/PBAT mainly occurred between 300 °C and 450 °C in one single step. The $T_{5\%}$ and T_{max} were 344.9 °C and 409.5 °C, respectively. The mass loss increased rapidly after increasing temperature, and the char residue left at 800 °C could be ignored. With the addition of 15 wt% PN-DOPO, the thermal decomposition of PEO/PBAT/PN-DOPO blends also showed a one-step mass loss, with the $T_{5\%}$ and T_{max} were 357.5°C and 409.7 °C, respectively. The residues slightly increased to 1.86 wt%. After adding Sep@$AlPO_4$ to PEO/PBAT, the onset thermal decomposition temperature increased to 356.8 °C, and the final residue was substantially increased to 10.27 wt%. These results are in agreement with other similar reported conclusions [25]. When PN-DOPO was combined with Sep@$AlPO_4$ into PEO/PBAT system, the thermal decomposition of the composites also exhibited the one-step mass loss, and the TGA and DTG curves of composites were similar with those for PEO/PBAT.

Preprints (www.preprints.org) | NOT PEER-REVIEWED | Posted: 9 November 2023 doi:10.20944/preprints202311.0666.v1

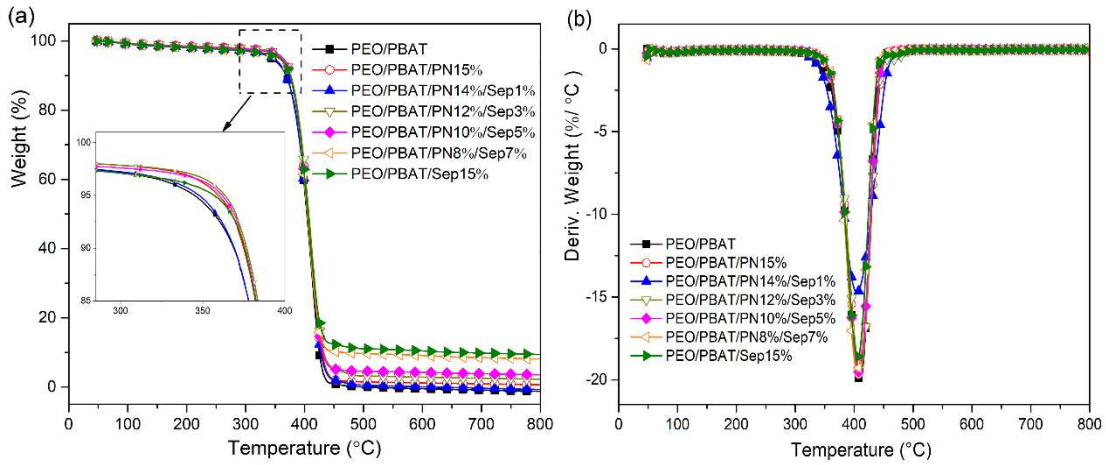

Figure 3. TGA (a) and DTG (b) curves of flame-retarded PEO/PBAT composites in nitrogen atmosphere.

As listed in Table 4, the apparent increases in $T_{5\%}$ implied the improvement in the initial thermal stability of PEO/PBAT with the combination of PN-DOPO and Sep@$AlPO_4$. Additionally, the char residues of composites were gradually increased by increasing the Sep@$AlPO_4$ contents. When the amount of Sep@$AlPO_4$ was 3 wt%, the composite had the highest $T_{5\%}$ and T_{max} of 363.4 °C and 410.7 °C, respectively. The $T_{5\%}$ increased by 18.5 °C and the char residue increased to 3.54 wt%, compared with the PEO/PBAT blend. The reasons for the improvement in initial thermal stability and char yield can be attributed to the synergistic effect of flame retardants and sepiolite on the formation of protective layers [36,37]. Consequently, the combination of PN-DOPO and Sep@$AlPO_4$ into PEO/PBAT may have a synergistic effect on the final residue, which can enhance the thermal stability of the samples and delay the emission of the decomposition products.

3.4. TGA-FTIR Analysis

The composition analysis of pyrolysis gas products can be conducted through TGA-FTIR testing. The three-dimensional TGA-FTIR spectrum of the thermal decomposition of PEO/PBAT, PEO/PBAT/PN15%, PEO/PBAT/PN10%/Sep5% and PEO/PBAT/Sep15% samples are shown in Figure 4a-d, respectively. Obviously, these samples all have similar characteristic bands in the regions of 1000-1300 cm^{-1}, 1600-1800 cm^{-1}, 2800-3000 cm^{-1} corresponded to the ester groups, carbonyl compounds and hydrocarbons, respectively. Figure 4(b) and (c) showed the several new bands compared to the spectrum in Figure 4(a) and (d). The new characteristic peaks at 700-1400 cm^{-1} could be attributed to the pyrolysis products of DOPO [25]. Furthermore, the intensity of peaks of PEO/PBAT and PEO/PBAT/Sep15% were weaker than those of PEO/PBAT/PN10%/Sep5%, indicating that the gas-phase effect of PEO/PBAT/PN-DOPO/Sep@$AlPO_4$ composites was superior to that of PEO/PBAT.

In order to explore the detailed changes of pyrolysis gas products during the thermal decomposition, the TGA-FTIR spectrum of PEO/PBAT, PEO/PBAT/PN15%, PEO/PBAT/PN10%/Sep5% and PEO/PBAT/Sep15% composites at the different decomposition temperature are expressed in Figure 5. For the four samples, the common characteristic absorption peaks appeared as follows: the hydrocarbons (2863 and 2966 cm^{-1}), carbonyl compounds (1745 cm^{-1}), aliphatic esters (1122, 1234 and 1265 cm^{-1}), C-O stretching vibration (1083 cm^{-1}) and C-H bending vibration (743 and 878 cm^{-1}) [1,8] when the temperature ranged from 380 °C to 440 °C. Moreover, the peaks at 3500–4000 cm^{-1} were ascribed to water. It could be seen from PBAT/PEO/PN15% sample, the peaks appeared at 1351 cm^{-1} and 1370 cm^{-1} attributed to the -P=O stretching variation. The absorption peaks at 1449 cm^{-1} corresponding to P-O-C_{Ar} were very weak at the temperature ranged from 400 °C to 600 °C [19,36]. It can be inferred that the volatiles of DOPO-based compounds were formed at the thermal decomposition process due to the introduction of PN-DOPO in the PEO/PBAT matrix. When the combination of PN-DOPO and Sep@$AlPO_4$ was added to PEO/PBAT, the absorption peaks appeared at 1351 cm^{-1} and 1370 cm^{-1} assigning to -P=O at the temperature ranged from 380 °C to 450 °C and

 doi:10.20944/preprints202311.0666.v1

1449 cm^{-1} corresponding to P-O-C_{Ar} bond appeared at 380 °C, respectively, comparing with PEO/PBAT and PEO/PBAT/Sep15% revealed in Figure 5 (a) and Figure 5 (d). These results indicated the introduction of Sep@$AlPO_4$ alone could not effectively increase gas-phase products. After the combination of PN-DOPO and Sep@$AlPO_4$ was added to PEO/PBAT, the blends exhibited the absorption peaks of phosphorous-containing groups and an increase in gas-phase volatiles during the thermal decomposition process, which suggested that a gas-phase flame-retardant mechanism for PEO/PBAT/PN-DOPO/ Sep@$AlPO_4$ composites played an important role in improving flame retardancy.

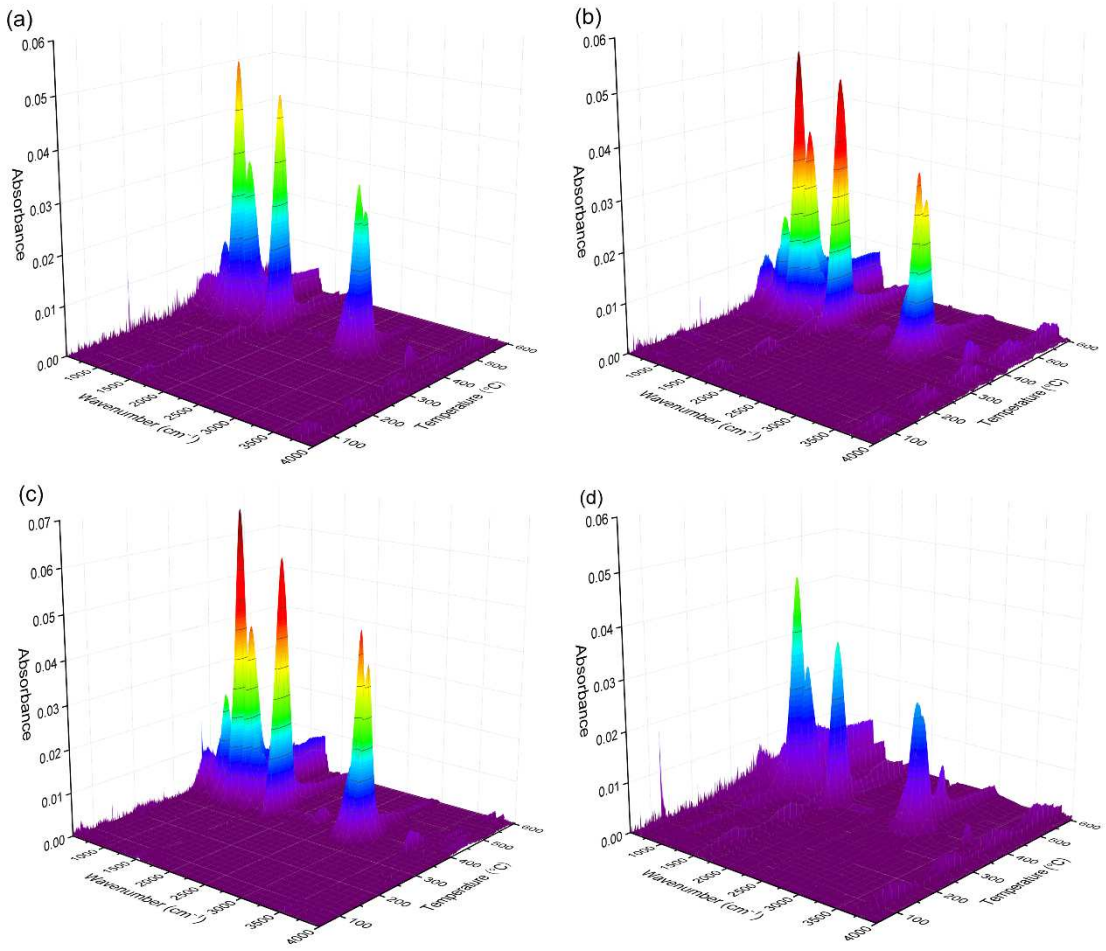

Figure 4. Three-dimensional TGA-FTIR spectrum of (a) PEO/PBAT, (b) PEO/PBAT/PN15%, (c) PEO/PBAT/PN10%/Sep5% and (d) PEO/PBAT/Sep15%.

Preprints (www.preprints.org) | NOT PEER-REVIEWED | Posted: 9 November 2023 doi:10.20944/preprints202311.0666.v1

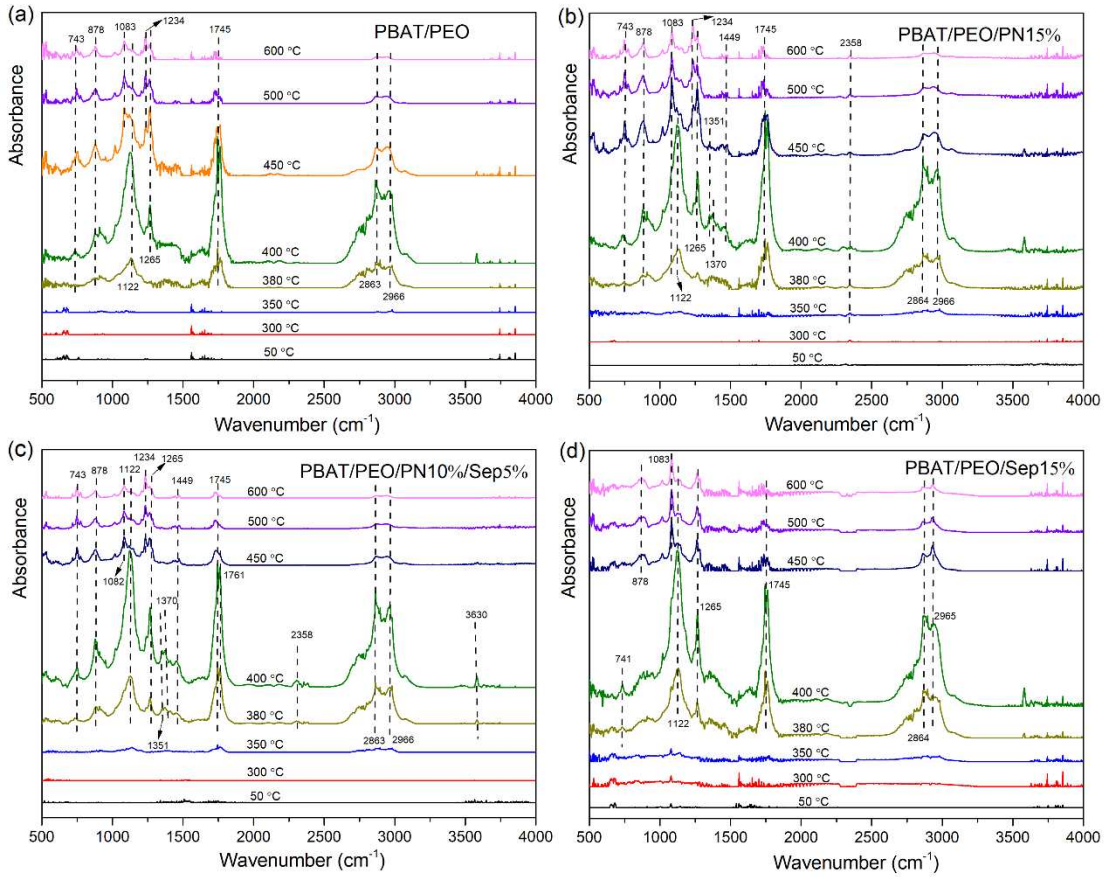

Figure 5. TGA-FTIR spectrum of the gaseous phase in the thermal decomposition for (a) PEO/PBAT, (b) PEO/PBAT/PN15%, (c) PEO/PBAT/PN10%/Sep5% and (d) PEO/PBAT/ Sep15% at different temperature.

3.5. Condensed-Phase Analysis

3.5.1. Macroscopic and Microscopic Morphologies of Residues

The macroscopic and microscopic morphologies of the char residues are explored in order to examine the specific flame-retardant mechanism for PEO/PBAT/PN-DOPO/ Sep@$AlPO_4$ composites in condensed phase. The digital photos of the char residues after the cone calorimeter tests are revealed in Figure 6. Figure 6(a) showed that the char residues left behind after the PEO/PBAT matrix combustion exhibited a discontinuous and loose structure, with some cracks and poor quality. With the incorporation of 15 wt% PN-DOPO, it could be observed in Figure 6(b) that the blends represented a very thin and incomplete char layer after burning. This form of residue could not protect the substrate from combustion or isolate the exchange of the combustion gases. With regard to PEO/PBAT/PN10%/Sep5% and PEO/PBAT/Sep15%, the morphologies of the residues differed substantially from those of PEO/PBAT and PEO/PBAT/PN15%, as expressed in Figure 6(c), (d). Especially for PEO/PBAT/PN10%/Sep5% composites, a complete, thick and dense residual carbon after combustion could be found in Figure 6(c). The results indicated that the combination of PN-DOPO and Sep@$AlPO_4$ could improve the quality and density of residual char, and played a role in the condensed-phase flame-retardant effect.

 doi:10.20944/preprints202311.0666.v1

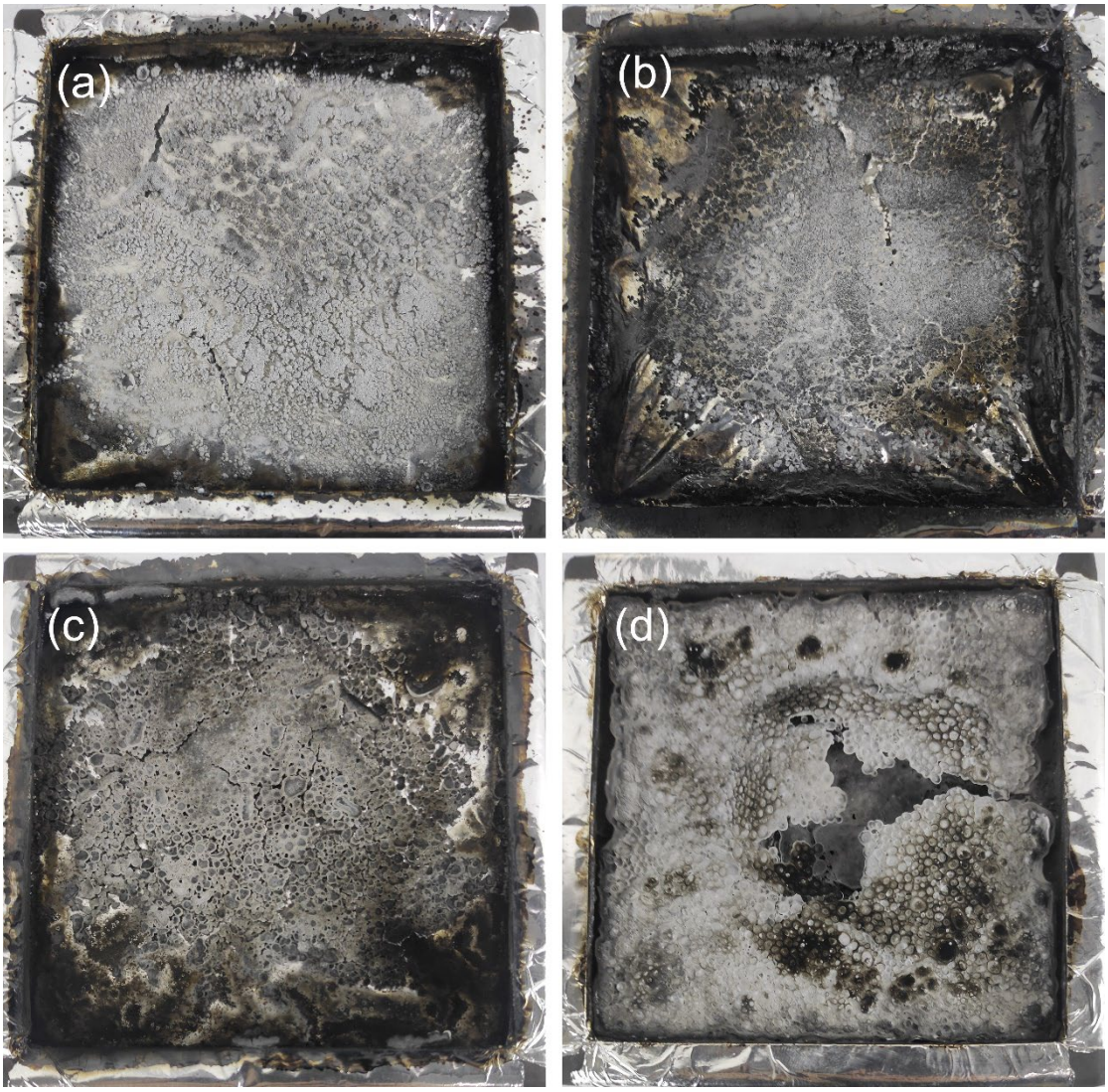

Figure 6. Digital photographs of the char residues after cone calorimeter tests for (a) PEO/PBAT, (b) PEO/PBAT/PN15%, (c) PEO/PBAT/PN10%/Sep5% and (d) PEO/PBAT/Sep15%.

The microscopic morphologies of char residues for the PEO/PBAT composites after cone calorimetry test are further observed by SEM. As shown in Figure 7(a), the char residue surface of pure PEO/PBAT matrix presented a relatively loose and inhomogeneous structure including some crevasses because of insufficient char formation during burning process. As for PEO/PBAT/PN15%, a uniform and dense char residues with a few holes after combustion could be found in Figure 7(b). With regard to PEO/PBAT/PN10%/Sep5% and PEO/PBAT/Sep15%, the morphologies of the char layer differed substantially from those of PEO/PBAT and PEO/PBAT/PN15%, as depicted in Figure 7(c) and (d). The surface morphologies of the char residues presented more continuous and compact fiberlike structure. The results indicated that the addition of Sep@$AlPO_4$ promoted the formation of higher char yield and phosphorus rich residues, resulting in a denser char layer [36,38]. The char layer had higher thermal stability and strength, which could effectively prevent the transfer of flammable volatiles and heat during the combustion, thereby further improving the flame retardancy of PEO/PBAT blends.

Preprints (www.preprints.org) | NOT PEER-REVIEWED | Posted: 9 November 2023 doi:10.20944/preprints202311.0666.v1

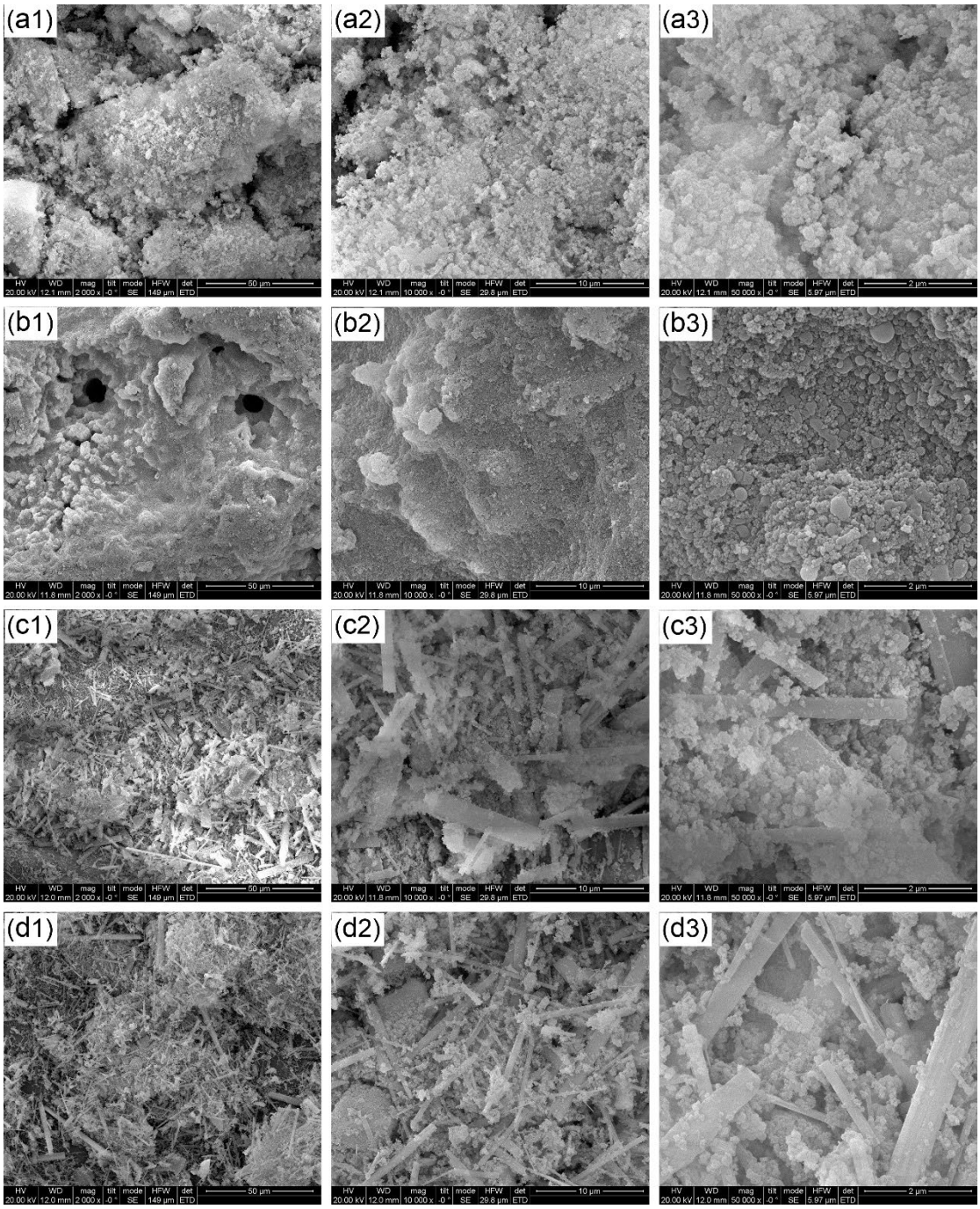

Figure 7. SEM images of the char residues after cone calorimeter tests for (a) PEO/PBAT (a1- 2000×, a2 - 10000×, a3 - 50000×), (b) PEO/PBAT/PN15% (b1- 2000×, b2 - 10000×, b3 - 50000×), (c) PEO/PBAT/PN10%/Sep5% (c1 - 2000×, c2 - 10000×, c3 - 50000×) and (d) PEO/PBAT/Sep15% (d1- 2000×, d2 - 10000×, d3 - 50000×).

3.5.2. Chemical Compositions of the Residues

The element compositions of the char residues after cone calorimeter tests are characterized by SEM-EDS, and the results of the char residues are displayed in Table 5. For the PEO/PBAT sample, only carbon and oxygen elements in the char residue were detected. There were 19.1 wt% phosphorus elements besides carbon and oxygen elements in the residue of PEO/PBAT/PN15% composites. The results illustrated phosphorus-containing products in the residues after the incorporation of DOPO-based flame retardants. While the oxygen, aluminum, silicon, magnesium elements and a relatively lower carbon content (11.7 wt%) and phosphorus content (12.8 wt%) were detected on the char layer

 doi:10.20944/preprints202311.0666.v1

of PEO/PBAT/Sep15% sample. These elements were the main components of aluminum phosphates and sepiolite residues [39,40]. After adding the combination of PN-DOPO and Sep@$AlPO_4$ into the PEO/PBAT blends, the sepiolite components (silicon, magnesium and aluminum) and an increase in the phosphorus content (21.2 wt%) were observed on the char residues. These further suggest PN-DOPO and Sep@$AlPO_4$ can catalyze the reactions to form phosphorus enriched and oxides chars, which exhibits a barrier effect to hinder the transfer of oxygen and heat.

Table 5. Element contents of the char residues of flame-retarded PEO/PBAT composites from the cone calorimeter via EDS.

Samples	Elemental Content (wt%)					
	C	O	P	Al	Si	Mg
PEO/PBAT	18.3	81.7	-	-	-	-
PEO/PBAT/PN15%	31.1	49.8	19.1	-	-	-
PEO/PBAT/PN10%/Sep5%	12.9	38.6	21.2	4.5	16.6	6.2
PEO/PBAT/Sep15%	11.7	37.5	12.8	5.5	23.1	9.4

In summary, the addition of PN-DOPO and Sep@$AlPO_4$ was added to PEO/PBAT blends. On the one hand, the composites exhibited an increase in gas-phase volatiles and the absorption peaks of phosphorous-containing products during combustion. On the other hand, the hybrid compounds rich in phosphorus, silicon, and aluminum oxides can promote a more continuous and dense carbon layer. In this case, the flame retardancy and thermal stability of PEO/PBAT system were significantly improved. Therefore, the PEO/PBAT/PN-DOPO/Sep@$AlPO_4$ composites exhibited a synergistic flame-retardant effect on gas-phase quenching effects and char formation in the condensed phase.

3.6. Rheological Behavior

Rheological measurements have recently been widely used to study the combustion behavior and flame retardancy of polymeric composites. The effects of melt flow characteristics on flame-retardant composites were investigated [24,41,42]. The influence of PN-DOPO and Sep@$AlPO_4$ compounds on the PEO/PBAT blends were examined. The relationship between storage modulus (G′), loss modulus (G″) as a function of the frequency (ω) for PEO/PBAT and flame retarded PEO/PBAT composites at 150 °C are illustrated in Figure 8, respectively. The G′ and G″ values of PEO/PBAT/PN-DOPO/ Sep@$AlPO_4$ composites were significantly higher than those of PEO/PBAT and PEO/PBAT/Sep@$AlPO_4$ blends over the whole frequency range. The G′ and G″ values increased with increasing Sep@$AlPO_4$ content with PEO/PBAT/PN-DOPO system. The increases in G′ and G″ of PEO/PBAT/PN-DOPO/Sep@$AlPO_4$ composites might be related to interfacial interactions, and both DOPO-based flame retardants and sepiolite could affect the viscoelastic behavior and relaxation of PEO/PBAT matrix [24,43,44]. Therefore, the addition of PN-DOPO and Sep@$AlPO_4$ increased the G′ and G″ values of the matrix. Among these samples, PEO/PBAT/PN8%/Sep7% sample showed the highest G′ and G″ values, suggesting that the interfacial interaction between PN-DOPO and PEO/PBAT matrix was improved by the immobilization of Sep@$AlPO_4$.

Preprints (www.preprints.org) | NOT PEER-REVIEWED | Posted: 9 November 2023 doi:10.20944/preprints202311.0666.v1

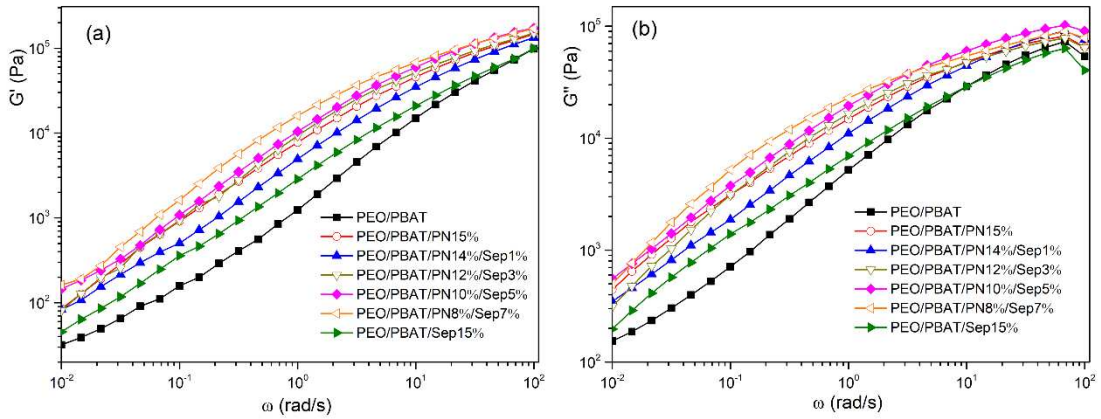

Figure 8. Storage modulus (a) and loss modulus (b) versus frequency of PEO/PBAT and flame-retarded PEO/PBAT composites.

Figure 9 shows the complex viscosity (η*) of PEO/PBAT and flame retarded PEO/PBAT composites. The η* value increased with increasing Sep@$AlPO_4$ content for PEO/PBAT/PN-DOPO/Sep@$AlPO_4$ system over the entire frequency range. The complex viscosity of PEO/PBAT/PN-DOPO/Sep@$AlPO_4$ composites were obviously higher than the those of PEO/PBAT and PEO/PBAT/Sep@$AlPO_4$ blends, which might be due to the presence of the network structure formed by flame retardants and inorganic particles [45]. The PEO/PBAT/PN8%/Sep7% sample had the highest η* value. The flame retarded PEO/PBAT/Sep@$AlPO_4$ composites high viscosity in the melted state, which could suppress the volatilization of decomposition products and limit the fluidity of polymer chains during combustion [24,46]. Additionally, high viscosity and modulus could also promote the cross-linking of condensed phases during the char formation, resulting in improvements in the flame retardancy of the composites.

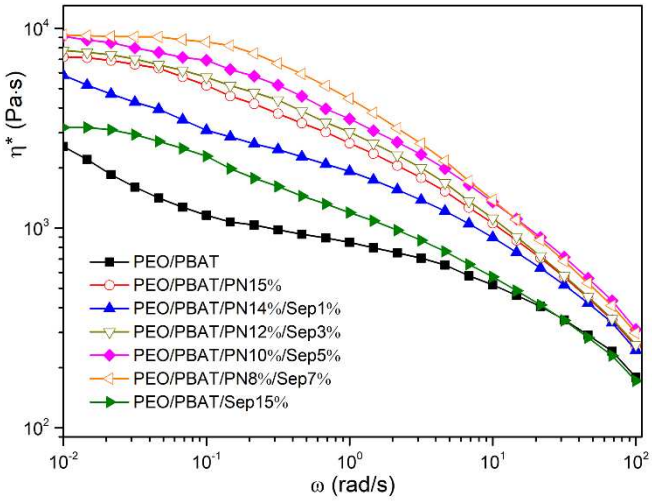

Figure 9. Complex viscosity versus frequency of PEO/PBAT and flame-retarded PEO/PBAT composites.

3.7. Mechanical Properties

The effect of PN-DOPO and Sep@$AlPO_4$ compounds on the mechanical properties of PEO/PBAT system was also investigated. Figure 10 shows the stress–strain curves and tensile strength, elongation at break, flexural strength as well as modulus of all samples. The tensile strength, flexural strength, flexural modulus and elongation at break of unfilled PEO/PBAT were 5.14 ± 0.21 MPa, 52.2 ± 1.94 MPa, 1.53 ± 0.05 GPa and 2.54 ± 0.09 %, respectively. At the addition of 15 wt% PN-DOPO, the tensile strength, flexural strength and modulus of the sample increased by 48.2%, 7.5% and 14.4%, respectively, whereas elongation at break remained almost unchanged. Incorporating the

Preprints (www.preprints.org) | NOT PEER-REVIEWED | Posted: 9 November 2023 doi:10.20944/preprints202311.0666.v1

combination of PN-DOPO and Sep@$AlPO_4$ had a positive effect on the mechanical of pure PEO/PBAT. It was found that the flexural strength, flexural modulus and elongation at break exhibited an obvious increase for PEO/PBAT/PN-DOPO/Sep@$AlPO_4$ composites compared with PEO/PBAT. With the incorporation of 10 wt% PN-DOPO and 5 wt% Sep@$AlPO_4$, the flexural strength, flexural modulus and elongation at break of PEO/PBAT/PN10%/Sep5% sample were increased by 19.9%, 51.6% and 892%, respectively, compared with neat PEO/PBAT. The improvement in flexural properties and elongation at break of flame-retarded PEO/PBAT composites may be due to the fact that PN-DOPO and Sep@$AlPO_4$ could be uniformly dispersed in the matrix during the melting process [24,47]. In addition, the elongation at break increased with the increasing Sep@$AlPO_4$ content, indicating that PN-DOPO/Sep@$AlPO_4$ compounds effectively improved the toughness of the matrix. Here, the multi-dimensional particle structure-polymer interfaces were well formed, which was conducive to load transfer from the polymer chain to the particles [48,49]. As a result, the higher mechanical properties could be discovered for PEO/PBAT/PN-DOPO/Sep@$AlPO_4$ composites.

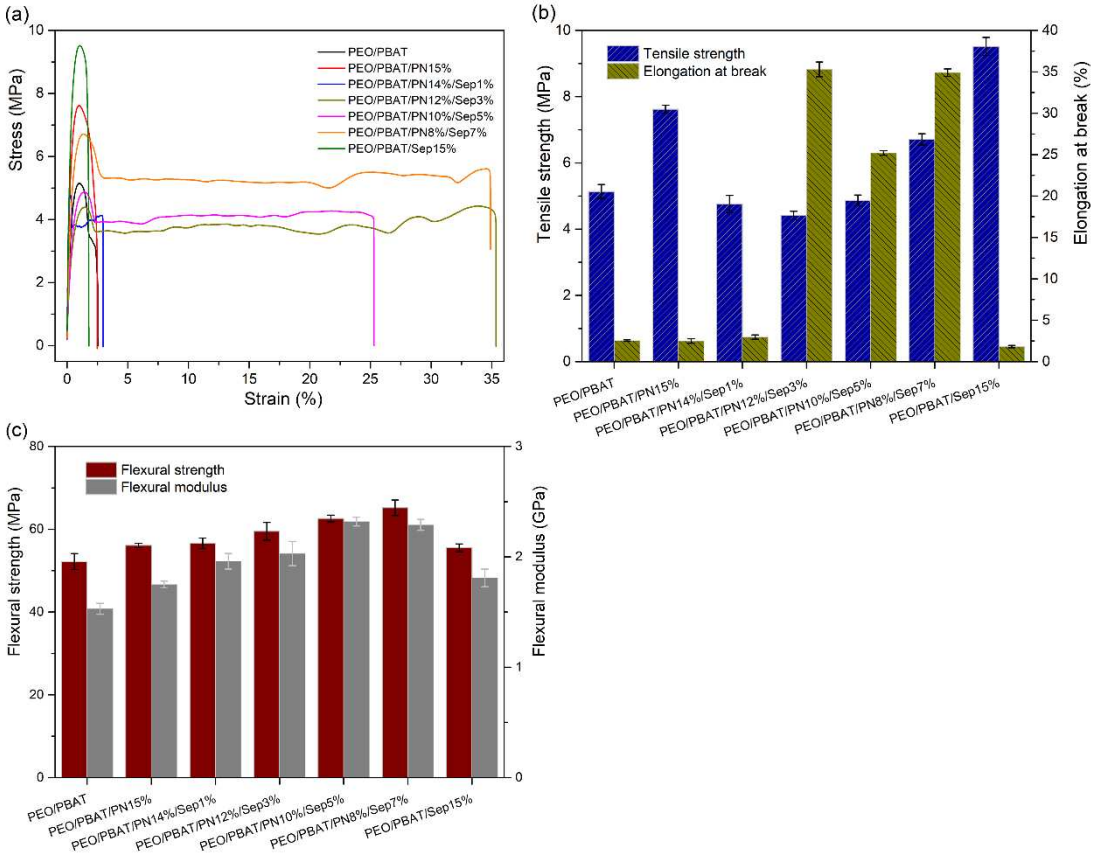

Figure 10. Mechanical properties of PEO/PBAT and flame-retarded PEO/PBAT composites, (a) stress-strain curves, (b) tensile strength and elongation at break, (c) flexural strength as well as modulus.

The mechanical properties of the composites mainly depend on the compatibility of the fillers in the matrix. To provide the evidence of the improved mechanical properties, SEM was used to observe the fracture surface of PEO/PBAT and flame-retarded PEO/PBAT composites. As given in Figure 11(a1-a3), PEO/PBAT showed a flat and smooth surface, which belonged to the typical brittle fracture of thermoplastic resin, indicating that plastic deformation did not occur during the fracture process [49,50]. For PEO/PBAT/PN15%, it also exhibited roughly the same cross-sectional characteristics as pure PEO/PBAT. This was consistent with the test results of mechanical properties. On the contrary, PEO/PBAT/PN8%/Sep7% composites presented rough surface with protrusions and pulling-out phenomena (see Figure 11c1-c3), which could be attributed to the interface interaction between the added fillers and the matrix. These obvious protrusions played an important role in hindering the propagation of microcracks [51]. In addition, the improvement of surface roughness validated the main fracture surface mode of plastic deformation, resulting in a significant increase in the elongation

 doi:10.20944/preprints202311.0666.v1

at break of PEO/PBAT/PN-DOPO/Sep@$AlPO_4$ composites. Moreover, PEO/PBAT/Sep15% also represented a rough surface with obvious protrusions and orientations, in its high-magnification SEM image (Figure 11d3), originating from the inorganic properties of fibrous sepiolite. Hence, PEO/PBAT/Sep15% sample exhibited the maximum tensile strength.

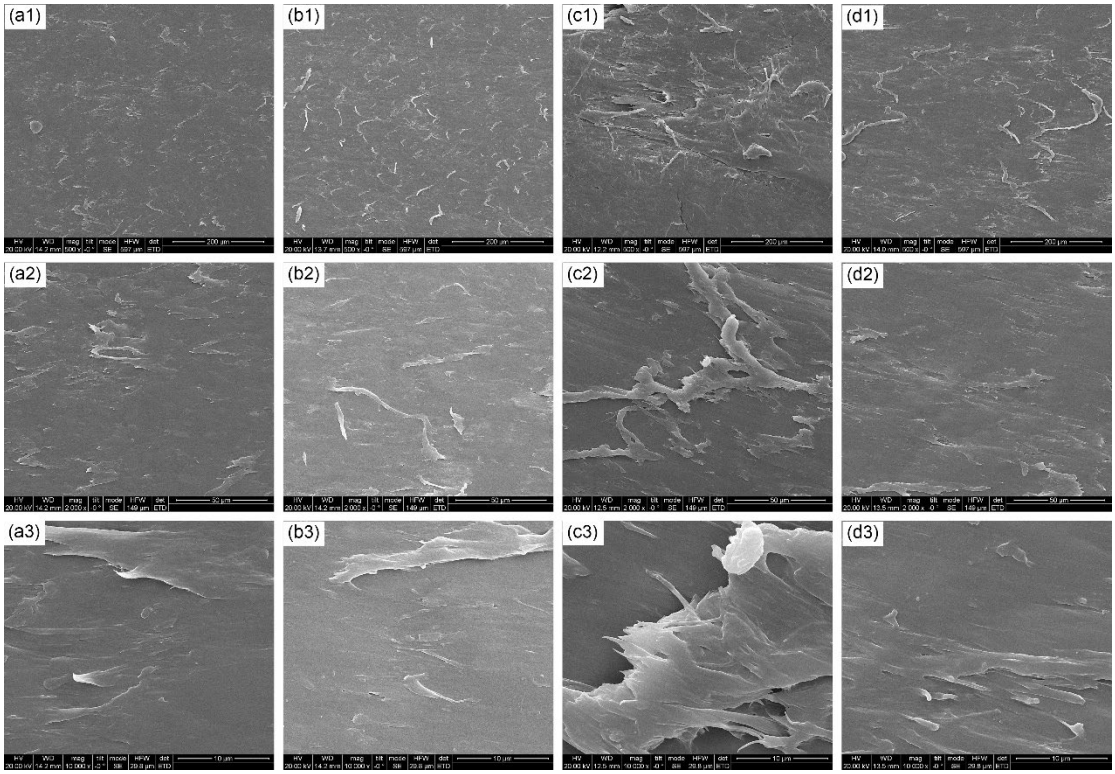

Figure 11. SEM images of fractured surfaces of PEO/PBAT (a1- 500×, a2 - 2000×, a3 - 10000×), PEO/PBAT/PN15% (b1- 500×, b2 - 2000×, b3 - 10000×), PEO/PBAT/PN10%/ Sep5% (c1 - 500×, c2 - 2000×, c3 - 10000×) and PEO/PBAT/Sep15% (d1- 500×, d2 - 2000×, d3 - 1000×) at different magnifications.

In summary, when PN-DOPO and modified sepiolite were applied to flame-retarded PEO/PBAT system, the composites exhibited the significant synergistic flame-retardant effects on combustion behavior, thermal stability, melt viscosity and carbonization. Additionally, compared with the PEO/PBAT, PEO/PBAT/PN-DOPO and PEO/PBAT/Sep@$AlPO_4$ system, the PEO/PBAT/ PN-DOPO/Sep@$AlPO_4$ composites also improved the mechanical properties such as elongation at break and flexural performance, exhibiting the plastic deformation cross-sectional characteristics.

4. Conclusions

In this work, DOPO-based flame retardant (PN-DOPO) in combination with aluminum phosphates coated sepiolite (Sep@$AlPO_4$) were jointly used to improve the flame retardancy and mechanical performance of PEO/PBAT system through melt mixing. The effects of PN-DOPO/Sep@$AlPO_4$ mixtures on the flame retardancy, thermal decomposition, carbonization and mechanical properties of the PEO/PBAT/PN-DOPO/Sep@$AlPO_4$ composites were systemically investigated using various analytical instruments. When adding 10 wt% PN-DOPO and 5 wt % Sep@$AlPO_4$, the LOI value of the composites was increased to 23.7% and the UL-94 test reached the V-1 rating. The p-HRR, THR and av-HRR values of PEO/PBAT/PN10%/Sep5% were reduced by 35.6%, 11.0% and 23.0% compared with those of PEO/PBAT, respectively. TGA results elucidated that the combination of PN-DOPO and Sep@$AlPO_4$ could enhance the initial thermal stability and char yield of PEO/PBAT system. In addition, TGA-FTIR tests indicated that PEO/PBAT/PN-DOPO/Sep@$AlPO_4$ blends exhibited the absorption peaks of phosphorous-containing groups and an increase in gas-phase volatiles during the thermal decomposition process. The results of SEM-EDS confirmed that PN-DOPO/Sep@$AlPO_4$ blends could promote a more continuous and dense carbon

layer rich in phosphorus, silicon, and aluminum oxides in the condensed phase. Moreover, PEO/PBAT/PN-DOPO/Sep@$AlPO_4$ composites exhibited the higher flexural properties and elongation at break than those of other samples. In conclusion, the combination of Sep@$AlPO_4$ with PN-DOPO presented an evident synergistic effect for flame-retardant PEO/PBAT materials, and Sep@$AlPO_4$ can be a highly promising and effective synergistic agent to simultaneously improve the flame retardancy, thermal stability and mechanical properties of flame-retarded PEO/PBAT blends.

Author Contributions: Methodology, W.H. and W.Y.; investigation, C.T. and Q.T.; formal analysis, K.W., C.Y. and X.X.; data curation, W.H., C.T. and C.M.; supervision, C.Y. and C.M.; writing—original draft preparation, W.H.; writing—review and editing, W.H., Q.T. and W.Y.; project administration, W.H. and W.Y. All authors have read and agreed to the published version of the manuscript.

Funding: This research was financially supported by the Natural Science Foundation of China (52063005), Innovation Group Project of Guizhou Provincial Department of Education (2020024), Guizhou Youth Science and Technology Talents Project (KY[2020]085), KY[2019]086, the Scientific Research Funds of Guiyang University (GYU-KY-2023), Discipline Master's Site Construction Project of Guiyang University by Guiyang City Financial Support Guiyang University (HC-2020), Science and Technology Support Project of Guizhou (2021488), Innovative Talent Project of Guizhou Province (2020004), Guizhou Provincial Talent Leadership office[2022]3 (The sixth batch of high-level innovative talents in Guizhou Province -Thousand-level talent) and Outstanding Young Science and Technology Talent Project of Guizhou Province (20215622).

Institutional Review Board Statement: Not applicable.

Informed Consent Statement: Not applicable.

Data Availability Statement: The data presented in this study are available on request from the corresponding author.

Conflicts of Interest: The authors declare no conflict of interest.

References

1. Liu, Y.Y.; Han, L.F.; Liao, C.; Yu, H.; Kan, Y.C.; Hu, Y. Ultra-thin, non-combustible PEO polymer solid electrolyte for high safety polymer lithium metal batteries. *Chem. Eng. J.* **2023**, *468*, 143222–143234.
2. Pongsuk, P.; Pumchusak, J. Effect of ultrasonication on the morphology, mechanical property, ionic conductivity, and flame retardancy of PEO-$LiCF_3SO_3$-halloysite nanotube composites for use as solid polymer electrolyte. *Polymers* **2022**, *14*, 3710–37225.
3. Jorge, L.; Meabe, L.; Riva, R.; Guzmán-González, G.; Porcarelliad, L.; Forsythade, M.; Mugica, A.; Müllerae, A.J.; Lecomte, P. Flame retardant polyphosphoester copolymers as solid polymer electrolyte for lithium batteries. *Polym. Chem.* **2021**, *12*, 3441–3450.
4. Fazli, A.; Rodrigue, D. Biosourced Poly (lactic acid)/polyamide-11 Blends: Effect of an Elastomer on the Morphology and Mechanical Properties. *Molecules* **2022**, *27*, 6819–6834.
5. Wang, K.; Jin, X.; He, X.H.; Huang, W.J.; Tian, Q.; Fu, Q.P.; Yan, W. Synthesis of aluminum phosphate-coated halloysite nanotubes: effects on morphological, mechanical, and rheological properties of PEO/PBAT Blends. *Nanomaterials* **2022**, *12*, 2896–2906.
6. Ye, A.; Wang, S.J.; Zhao, Q.; Wang, Y.M.; Liu, C.T.; Shen, C.Y. Poly (ethylene oxide)-promoted dispersion of graphene nanoplatelets and its effect on the properties of poly (lactic acid)/poly (butylene adipate-co-terephthalate) based nanocomposites. *Mater. Lett.* **2019**, *253*, 34–37.
7. Qi, J.; Pan, Y.T.; Luo, Z.L.; Wang, B.B. Facile and scalable fabrication of bioderived flame retardant based on adenine for enhancing fire safety of fully biodegradable PLA/PBAT/TPS ternary blends. *J. Appl. Polym. Sci.* **2021**, *138*, 50877–50893.
8. Li, X.J.; Cai, Z.Z.; Wang, X.; Zhang, Z.; Tan, D.Y.; Xie, L.; Sun, H.J.; Zhong, G.J. The combined effect of absorption and catalysis of halloysite nanotubes during the thermal degradation of PBAT nanocomposties. *Appl. Clay Sci.* **2020**, *196*, 105762–105770.
9. Liu, X.Q.; Zhang, C.; Gao, S.Y.; Cai, S.J.; Wang, Q.F.; Liu, J.Y.; Liu, Z.H. A novel polyphosphonate flame-retardant additive towards safety-reinforced all-solid-state polymer electrolyte. *Mater. Chem. Phys.* **2020**, *239*, 122014–122021.
10. Wang, Y.R.; Fang, T.M.; Wang, S.Y.; Wang, C.; Li, D.H.; Xia, Y.Z. Alginate fiber-grafted polyetheramine-driven high ion-conductive and flame-retardant separator and solid polymer electrolyte for lithium metal batteries. *ACS Appl. Mater. Interfaces* **2022**, *14*, 56780–56789.

11. Phetwarotai, W.; Suparanon, T.; Phusunti, N.; Potiyaraj, P. Influence of compatibilizer and multifunctional additive loadings on flame retardation, plasticization, and impact modification of polylactide and poly (butylene adipate-co-terephthalate) biodegradable blends. *Polym. Advan. Technol.* **2020**, *31*, 2094–2107.
12. Zhou, Y.; Qiu, S.; Waterhouse, G.I.N.; Zhang, K.; Xu, J. Enhancing the properties of PBAT/PLA composites with novel phosphorus-based ionic liquid compatibilizers. *Mater. Today Commun.* **2021**, *27*,102407–102416.
13. Chen, L.; Li, Y.T.; Fan, S.P.; Nan, C.W.; Goodenough, J.B. PEO/garnet composite electrolytes for solid-state lithium batteries: from "ceramic-in-polymer" to "polymer-in-ceramic". *Nano Energy* **2018**, *46*, 176–184.
14. Nascimento, M.; Novais, S.; Ding, M.S.; Ferreira, M.S.; Koch, S.; Passerini S.; Pinto, J.L. Internal strain and temperature discrimination with optical fiber hybrid sensors in Li-ion batteries. *J. Power Sources* **2019**, *410*, 1–9.
15. Zhai, H.W.; Xu, P.Y.; Ning, M.Q.; Cheng, Q.; Mandal, J.; Yang, Y. A flexible solid composite electrolyte with vertically aligned and connected ion-conducting nanoparticles for lithium batteries. *Nano Lett.* **2017**,*17*, 3182–3187.
16. Han, L.; Liao, C.; Mu, X.; Wu, N.; Xu, Z.; Wang, J.W.; Song, L.; Kan, Y.C.; Hu, Y. Flame-retardant ADP/PEO solid polymer electrolyte for dendrite-free and long-life lithium battery by generating Al, P-rich SEI layer. *Nano Lett.* **2021**, *21*, 4447–4453.
17. Salmeia, K.A.; Gaan, S. An overview of some recent advances in DOPO-derivatives: Chemistry and flame retardant applications. *Polym. Degrad. Stabil.* **2015**, *113*, 119–134.
18. Levchik, S.; Piotrowski, A.; Weil, E.; Yao, Q. New developments in flame retardancy of epoxy resins. *Polym. Degrad. Stabil.* **2005**, *46*, 2778–2788.
19. Huang, W.J.; He, W.T.; Long, L.J.; Yan, W.; He, M.; Qin, S.H.; Yu, J. Highly efficient flame-retardant glass-fiber-reinforced polyamide 6T system based on a novel DOPO-based derivative: Flame retardancy, thermal decomposition and pyrolysis behavior. *Polym. Degrad. Stabil.* **2018**, *148*, 26–41.
20. Zhou, Y.; Lin, Y.; Tawiah, B.; Sun, J.; Yuen, R.K.K.; Fei, B. DOPO-decorated two-dimensional mXene nanosheets for flame-retardant, ultraviolet-protective, and reinforced polylactide composites. *ACS Appl. Mater. Interfaces* **2021**, *13*, 21876−21887.
21. Huang, W.J.; Yan W.; He W.T., Wang K.; Long L.J.; He M.; Yu J. Synergistic flame-retardant effect of DOPO-based derivative and organo-montmorillonite on glass-fiber-reinforced polyamide 6 T. *Polym. Advan. Technol.* **2020**, *31*, 2083–2093.
22. Yan, W.; Yu, J.; Zhang, M.Q.; Wang, T.; Wen, C.; Qin, S.H.; Huang W.J. Effect of multiwalled carbon nanotubes and phenethylbridged DOPO derivative on flame retardancy of epoxy resin. *J. Polym. Res.* **2018**, *25*, 72–79.
23. Long, L.J.; Chang, Q.F.; He, W.T.; Xiang, Y.S.; Qin, S.H.; Yu, J. Effects of bridged DOPO derivatives on the thermal stability and flame retardant properties of poly (lactic acid). *Polym. Degrad. Stabil.* **2017**, *139*, 55–66.
24. Huang, W.J.; Wang, K.; Tu, C.Y.; Xu, X.L.; Tian, Q.; Ma, C.; Fu, Q.P.; Yan, W. Synergistic effects of DOPO-based derivative and organo-montmorillonite on flame retardancy, thermal stability and mechanical properties of polypropylene. *Polymers* **2022**, *14*, 2372–2388.
25. Jiang, P.; Zhang, S.; Bourbigot, S.; Chen, Z.; Duquesne, S.; Casetta, M. Surface grafting of sepiolite with a phosphaphenanthrene derivative and its flame-retardant mechanism on PLA nanocomposites. *Polym. Degrad. Stabil.* **2019**, *165*, 68–79.
26. Beryl, J.R.; Xavier, J.R. Halloysite for clay-polymer nanocomposites: effects of nanofillers on the anti-corrosion, mechanical, microstructure, and flame-retardant properties- a review. *J. Mater. Sci.* **2023**, 58, 10943–10974.
27. Hu, Y.L.; Feng, D.; Xie, Y.H.; Xie, D.L. Microwave-assisted confining flame-retardant polypropylene in carbon nanotube conductive networks for improved electromagnetic interference shielding and flame retardation. *Adv. Eng. Mater.* **2021**, *23*, 2100024–2100031.
28. Pan, Y.; Liu, L.X.; Cai, W.; Hu, Y.; Jiang, S.D.; Zhao, H.T. Effect of layer-by-layer self-assembled sepiolite-based nanocoating on flame retardant and smoke suppressant properties of flexible polyurethane foam. *Appl. Clay Sci.* **2019**, *168*, 230–236.
29. Pappalardo, S.; Russo, P.; Acierno, D., Rabe, S., Schartel, B. The synergistic effect of organically modified sepiolite in intumescent flame retardant polypropylene. *Eur. Polym. J.* **2016**, *76*, 196–207.
30. Yan, W.; Xie, P.; Yang, Z.W.; Luo, G.J.; Huang, W.J.; Tian, Q.; Tu, C.Y.; Zhang, C.M.; Yang, C.L.; Wang, K. Flame-retardant behaviors of aluminum phosphates coated sepiolite in epoxy resin. *J. Fire Sci.* **2021**, *39*, 3–18.
31. Huang, W.J.; He, W.T.; Long, L.J.; Yan, W.; He, M.; Qin, S.H.; Yu, J. Thermal degradation kinetics of flame-retardant glass-fiber-reinforced polyamide 6T composites based on bridged DOPO derivatives. *Polym. Bull.* **2019**, *76*, 2061–2080.
32. Samyn, F.; Bourbigot, S. Protection mechanism of a flame-retarded polyamide 6 nanocomposite. *J. Fire Sci.* **2014**, *32*, 241–256.
33. Zhang, W.C.; Li, X.M.; Li, L.M.; Yang, R.J. Study of the synergistic effect of silicon and phosphorus on the blowing-out effect of epoxy resin composites. *Polym. Degrad. Stabil.* **2012**, *97*, 1041–1048.

34. Yuan, B.; Fan, A.; Yang, M.; Chen, X.F.; Hu, Y.; Bao, C.L.; Jiang, S.H.; Niu, Y.; Zhang, Y. The effects of graphene on the flammability and fire behavior of intumescent flame retardant polypropylene composites at different flame scenarios. *Polym. Degrad. Stabil.* **2017**, *143*, 42–56.
35. Fang, Y.Y.; Qian, L.J.; Huang, Z.G.; Tang, S.; Qiu, Y. Synergistic charring effect of triazinetrione-alkylphosphinate and phosphaphenanthrene derivatives in epoxy thermosets. *RSC Adv.* **2017**, *73*, 46505–46513.
36. Zhan, Z.S.; Xu, M.J.; Li, B. Synergistic effects of sepiolite on the flame retardant properties and thermal degradation behaviors of polyamide 66/aluminum diethylphosphinate composites. *Polym. Degrad. Stabil.* **2015**, *117*, 66–74.
37. Zhang, H.J.; Hu, X.P.; Liu, Y.R.; Zhang, S.H.; Wu, Z.Z. Convenient synthesis of one-dimensional a-SEP@LDH via self-assembly towards simultaneously improved fire retardance, mechanical strength and thermal resistance for epoxy resin. *Compos. Part B-Eng.* **2021**, *216*, 108857–108873.
38. Shafi, U.R.; Sana, J.; Muhammad, S.; Iftikhar, H.G.; Badar, R.; Muhammad, N.; Sabrina J.C. Polystyrene-sepiolite clay nanocomposites with enhanced mechanical and thermal properties. *Polymers* **2022**, 14, 3576–3589.
39. Xu, T.; Qian, D.; Hu, Y.; Zhu, Y.Z.; Zhong, Y.; Zhang, L.P.; Xu, H.; Peng, H.X.; Mao, Z.P. Effect of Sepiolite-Loaded Fe_2O_3 on Flame Retardancy of Waterborne Polyurethane. *Adv. Polym. Tech.* **2021**, *2021*, 1–10.
40. Wu, N.J.; Xiu, Z.X. Surface microencapsulation modification of aluminum hypophosphite and improved flame retardancy and mechanical properties of flame-retardant acrylonitrile–butadiene–styrene composites. *RSC Adv.* **2015**, *61*, 49143–49152.
41. Cheng, B. F.; Li, X.M.; Hao, J.W.; Yang, R.J. Rheological behavior of polycarbonate/ ultrafine octaphenyl silsesquioxane (OPS) composites. *J. Appl. Polym. Sci.* **2016**,*133*, 43638–43649.
42. Zhu, F.; Yasin, S.; Hussain, M. Viscoelastic Rheological Behaviors of Polypropylene and LMPP Blends. *Polymers* **2021**, *13*, 3485–3495.
43. Bascucci, C.; Duretek, I.; Lehner, S.; Holzer, C.; Gaan, S.; Hufenus, R.; Gooneie, A. Investigating thermomechanical recycling of poly (ethylene terephthalate) containing phosphorus flame retardants. *Polym. Degrad. Stabil.* **2021**, *195*, 109783-109791.
44. Wang, L.; Wang, G.; Liu, Z.; Xu, S.M.; Wang, Y.Z. Rheological premonitory of nanoclay morphology on the mechanical characteristics of composite aerogels. *Compos. Part B-Eng.* **2019**, *173*, 106889–106895.
45. Li, X.; Liang, D.; Hu, Z, He, J.L.; Bian, X.C.; Cui, J.L. Synergistic effects of polyoxometalate-based ionic liquid-doped sepiolite in intumescent flame-retardant high-density polyethylene. *Polym. Advan. Technol.* **2021**, *32*, 2240–2251.
46. He, W.T.; Liao, S.T.; Xiang, Y.S.; Long, L.J.; Qin, S.H.; Yu, J. Structure and properties study of PA6 nanocomposites flame retarded by aluminium salt of diisobutylphosphinic acid and different organic montmorillonites. *Polymers* **2018**, *10*, 312–321.
47. Zhou, X.; Qiu, S.; Xing, W.; Gangireddy, C.S.R.; Gui, Z.; Hu, Y. Hierarchical polyphosphazene@ molybdenum disulfide hybrid structure for enhancing the flame retardancy and mechanical property of epoxy resins. *ACS Appl. Mater. Interfaces* **2017**, *9*, 29147–29156.
48. Jia, P.; Zhu, Y.; Lu, J.; Wang, B.; Song, L.; Wang, B.; Hu, Y. Multifunctional fireproof electromagnetic shielding polyurethane films with thermal management performance. *Chem. Eng. J.* **2022**, *439*, 135673–135681.
49. Cao, Y.; Wang, Z.; Wang, J.; Wei, Y.; Yu, S. Chitosan-bridged synthesis of 2D/2D hierarchical nanostructure towards promoting the fire safety and mechanical property of epoxy resin. *Compos. Part A-Appl. Sci.* **2022**, *158*, 106958–106969.
50. Li, Z.; Chen, M.; Li, S.; Fan, X.M.; Liu, C.P. Simultaneously improving the thermal, flame retardant and mechanical properties of epoxy resins modified by a novel multi-element synergistic flame retardant. *Macromol. Mater. Eng.* **2019**, *304*, 1800619–1800627.
51. Jian, R.; Wang, P.; Xia, L.; Yu, X.Q.; Zheng, X.L.; Shao, Z.B. Low-flammability epoxy resins with improved mechanical properties using a Lewis base based on phosphaphenanthrene and 2-aminothiazole. *J. Mater. Sci.* **2017**, *52*, 9907–9921.